

Measurement of Gasoline Spray Propagation by means of Synchrotron X-Ray

Y. Yue, C. Powell, R. Cuenca, R. Poola*, J. Wang
Argonne National Laboratory, Argonne, IL 60439

Scott E. Parrish
General Motors, Warren, MI 48090

Abstract

A quantitative and time-resolved radiographic technique has been used to characterize hollow-cone gasoline sprays in the near-nozzle region. The highly penetrative nature of x-rays promises the direct measurements of dense sprays that are difficult to study by visible-light based techniques. Time-resolved x-radiography measurement enables us to map the mass distribution near the spray nozzle, even immediately adjacent to the orifice. The quantitative nature of the measurement also permits the re-construction of spray structure and the progress of the spray development. It is observed that the speed of fuel injected in the later part of the injection is higher than injected earlier and that the initial fuel speed variation caused the spray plume to be compressed in space.

INTRODUCTION

With increasing demand on higher automotive fuel economy and lower exhaust emissions, the need of developing better injection system has become more urgent than ever. Recent research has demonstrated that gasoline direct injection technique is a promising technology for future light-duty gasoline vehicles. It is well known that in direct injection gasoline engines, the spray characteristics and mixing process play a very important role in the combustion process. Understanding gasoline spray characteristics is important for designing effective injectors and injection systems. It is also vital to achieve realistic computational modeling. To ensure high combustion efficiency and low emissions, well-atomized sprays and proper spray penetration are always required over the entire GDI engine operating range [1, 2]. Despite significant advances in laser diagnostics over the last 20 years [3-10], the region close to the nozzle has remained impenetrable by visible light, and so quantitative data about this region are generally lacking. In this region, heavy concentration of fuel droplets prevents visible light from penetrating and limits quantitative evaluations of the sprays.

X-rays are highly penetrative in low-atomic-number materials even when they consist of extremely dense droplets. The x-ray technique utilizing line-of-sight absorption of monochromatic synchrotron x-rays can measure the fuel mass with high temporal and spatial resolution [11-14]. The lower scattering cross-section of fuel in the x-rays regime allows direct measurements of spray structure that are difficult with other visible-light-

based optical techniques. With the quantitative nature of the measurement, the instantaneous fuel mass in the beam can be determined accurately based on the x-ray transmission data and the calibration of the mass absorption coefficient. Quantitative spray images and spray development can be reconstructed with the measured two-dimensional (2-D) projection of fuel mass distribution.

Because of the high intensity of x-ray beams from synchrotron sources, it is possible to select a narrow bandwidth of x-ray energies. The high monochromaticity of the x-ray beam results in a straightforward relationship between the measured x-ray transmission and the mass of fuel in the path of the beam. For monochromatic x-rays transmitted through a non-uniformly distributed material, the attenuation due to the sample is characterized by

$$I/I_0 = \exp(-\mu_M M), \quad (1)$$

where I and I_0 are transmitted and incident x-ray intensities, respectively. μ_M is the mass absorption coefficient and M is the total mass in the beam. With precise calibration of μ_M , the x-ray absorption technique can determine absolute mass, M , in the beam path.

EXPERIMENTAL ASPECTS

A production gasoline fuel injection system with an outwardly opening injector was employed. Test fuel (Viscor® calibration fluid) was injected into a chamber filled with an inert gas (nitrogen) at atmospheric pressure and room temperature. The spray chamber (38 cm long,

* Current address: Electro-Motive Div. of GM, LaGrange, IL-60525

5 cm wide, and 12 cm tall) was a simple box that was designed to hold the injector, contain the spray plume, and allow nitrogen gas to scavenge the fuel vapors. The spray chamber had windows 50 mm long and 25 mm wide that provide line-of-sight access for the x-rays. Polymer films were used for the beam entrance and exit windows, which allowed x-ray access to the fuel spray. The fuel used in this study blended with a commercially available cerium-containing compound. The blend had a cerium concentration of about 4.2% by weight. A gasoline injection system with outwardly-opening injector was employed in this experiment. Table 1 provides a summary of the injection system, test fuel, and test conditions employed for the x-ray absorption measurements.

Table 1 Test Conditions

Parameters	Quantity
No. of orifices	1
Orifice diameter, mm	2.0
Fill gas	N ₂
Fill gas pressure, MPa	0.1
Fill gas temperature, °C	25 to 30
Fuel	Viscor and Ce -containing additive
Specifi. Gravity, kg/m ³	840.5

The time-resolved radiography experiments were performed at SRI-CAT bending magnet beamline 1-BM of the Advanced Photon Source (APS), Argonne National Laboratory (ANL). A schematic of the x-ray absorption setup for studying the gasoline sprays is shown in Figure 1. The x-ray beam was focused and collimated by a pair of X-Y slits to a size of 140 μm (horizontal, H) × 50 μm (vertical, V). These numbers represent the spatial resolution of the measurement. Smaller beam area, such as 25 μm (H) × 25 μm (V), can be achieved if desirable. Because of the small beam size, a scan through the entire spray was necessary to image the spray. More information about the x-ray experimental setup has been given in our previous publications [11-14].

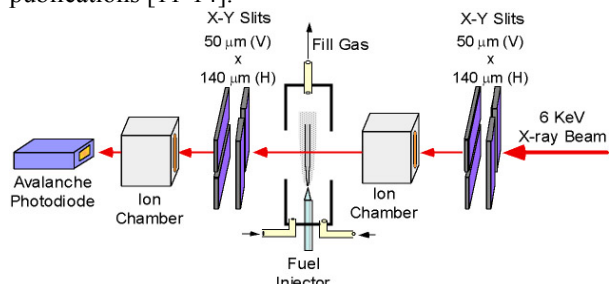


Figure 1 Schematic of experimental test setup

The calibration process based on Equation 1 yielded $\mu_M = 522 \text{ mg}^{-1}$ for the x-ray beam used in the experiment. The uncertainty of the calibration process was determined by successive trials to be ~1.5%. This reflects the systematic error of the mass calibration.

A TTL trigger signal was used to activate the fuel injection and data acquisition system. There is a time delay between the beginning of the injection and the pulse to drive the nozzle opening solenoid. The transmission signal was averaged for 100 cycles in order to improve the signal/noise ratio of the data.

RESULTS AND DISCUSSION

The following convention is used for clarity. The spray axis is defined as *x*-axis, while the *y*-axis is perpendicular to *x*-axis and the x-ray beam, and *z*-axis is along the beam direction. The origin is at the center of nozzle tip.

The instantaneous mass in the beam can be accurately evaluated on the basis of measured x-ray transmission and the mass calibration by Equation 1. The time-resolved x-ray transmission and the calculated mass of fuel in the beam measured at *x*=2 mm and *y*=2.22 mm are shown in Figure 2. These plots depict the typical features of the absorption measurements. In this particular measurement case, at the very beginning (*t* < 0.23 ms), the fuel has not yet reached the measuring point, and the x-ray transmission is near 1. This region of the plot serves to determine the 100% transmission condition. At a later time (*t* = 0.24 ms), the fuel intersects the x-ray beam, and a sharp decrease appears in the transmission, indicating a well-defined boundary between ambient gas and fuel spray. An oscillation can clearly be seen in the plot during injection, which shows that the injection pressure and rate is unsteady. At even later times (*t* = 0.8 ms), the trailing edge appears as the fuel exits the x-ray beam and the transmission nearly returns to the baseline value. The small peak in the later stage (1.2ms) revealed that there was a minor second injection attributable to the bounce of injector nozzle.

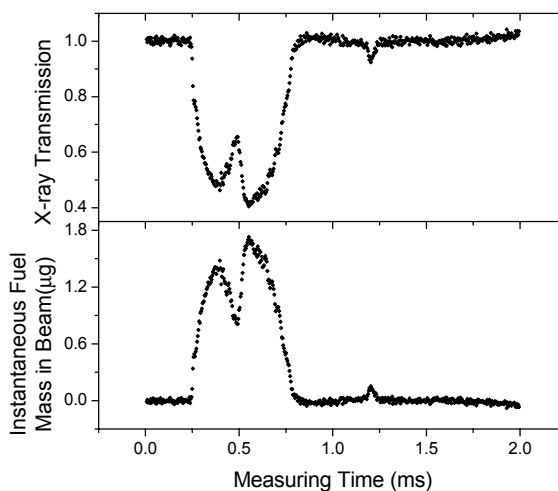


Figure 2 Time-resolved x-ray transmission and fuel mass (at *x* = 2 mm, *y* = 2.22 mm).

Given the high temporal and spatial resolution of x-ray measurement, the process of spray development and instantaneous mass distribution in spray can be analyzed in great detail. The image in Figure 3 is reconstructed on the basis of point-by-point measurements of 1600 positions at 0.442ms from the start of injection. The gray-scale represents the total instantaneous mass in the beam. The measuring distance between these sampling points ranged from 25 μm to 100 μm in the radial direction and 1 mm in the axial direction. The minimum mass amount that can be detected by this method was dictated by the signal-to-noise ratio (approximated 2% of transmission value) in the data collection.

The spray development process can be analyzed based on the quantitatively reconstructed spray images and mass distribution. The distinctive difference between traditional optical methods and the monochromatic x-ray radiography is that x-ray images contain highly quantitative information such as the fuel mass distribution and fuel concentration.

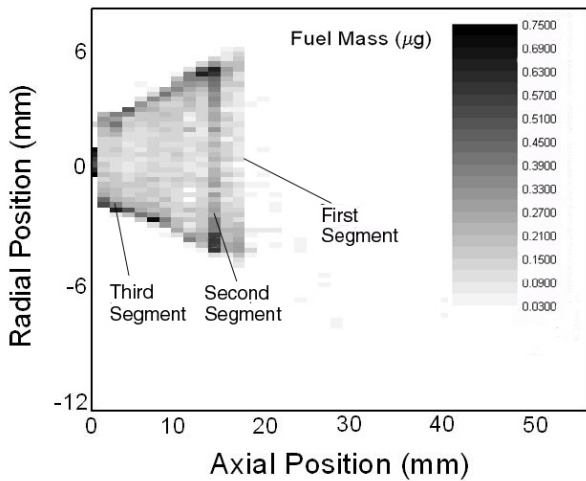


Figure 3 Reconstructed snapshots of 2-dimensionally projected mass distributions at 0.48 ms after injection.

It was observed in reconstructed images that the spray cone was formed quickly after the nozzle opened and the full spray cone angle remains steady at about 24° during the injection period. In Figure 3, a number of differentiated segments can be observed (dark color strips perpendicular to the spray axis). The first segment in the leading edge, the second and third inside spray plume. Figure 4 shows the comparison of instantaneous mass in the beam at different locations inside the spray. The three peaks in the curves relate to three different segments in Figure 3. It can be seen that during the development process of the spray the relative positions of segments were quite dynamic. The second segment caught up with the first one (in leading edge) and gradually merged into the spray leading edge. The third segment was moving close to the second. The penetration curves of each fuel segment are shown in Figure 5. The time delay for each indicates that the fuel in those segments originated at different injection time instances and the speeds were significantly different. The

second segment continuously traveled much faster and finally caught up with the spray leading edge at around 20~25 mm away from the nozzle.

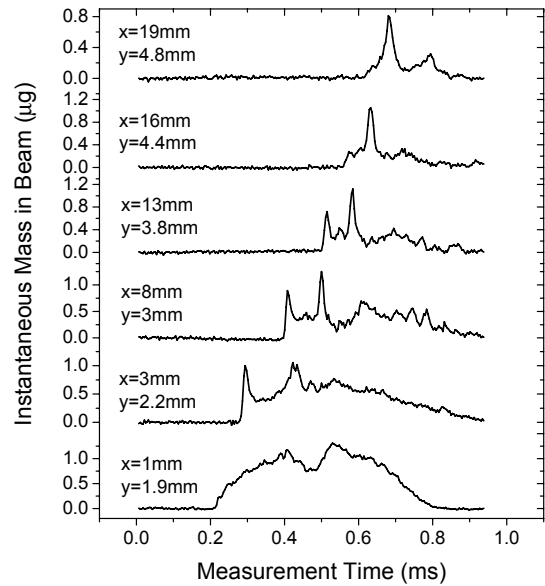


Figure 4 Comparison of instantaneous mass in beam at different locations near the edge of the hollow-cone.

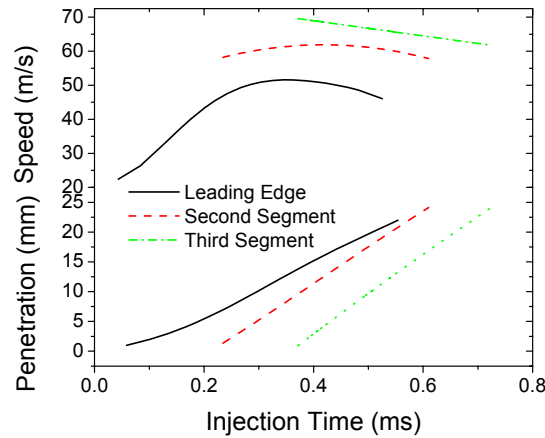


Figure 5 Penetration of spray leading edge and high dense areas and their speed comparison.

The speeds of the fuel segments in the spray are also shown in figure 5. Before the fuel in the second segment merged with the first one (see Figure 6), it had greater speed. The leading edge increases speed in the first 0.3 ms after the injection but it decrease later on. The second segment increased its speed slightly from 57 m/s to 63 m/s and then decreased in a slow rate with a speed value. The speed of the third segment is the highest, although it decreased immediately after exciting from the nozzle.

The first part of the spray was presumable injected under lower pressure, hence, it traveled at lower speed values. Upon impact onto the ambient gas, the leading edge of the spray slows down, and the portion behind the leading

edge emerged as new leading edge. Since the later portion of the spray was injected under more steady and possibly increasing pressure, the later portion transfer momentum to the front part of the spray. Therefore, the ‘apparent’ speed of the first increased as a function of time and the speed should be considered as ‘phase’ speed as opposed to the true speed of fuel particles. Because the third segment was near the end of injection duration, there was no substantial momentum transfer occurring after the injection. Therefore, this part of the fuel jet exited nozzle in higher speed and the speed. On the other hand, the second segment was in a much balanced momentum transfer situation: it increased its speed in the beginning due to positive momentum transfer from the fuel behind the segment and then decreased due to transferring momentum to fuel the fuel segment with lower speed in front of it. Therefore, the hollow-cone spray studied here, the speed of fuel injected later is faster than earlier and causes the spray compression in the axial direction while traveling in the ambient gas environment.

SUMMARY

In this paper, a quantitative study of a gasoline spray by means of monochromatic x-ray radiography is presented.

The speed of spray leading edge increased its speed in the beginning of the injection (<about 0.3ms) and then decreased after 25 mm away from nozzle. Due to the highly-penetrative nature of x-rays, this technique not only detects the leading edge speed by also probes internal dynamics of the sprays. The results have demonstrated unambiguously that the fuel speed gradient over a wide range existed inside the spray. The speed of fuel injected later in spray was faster, which clearly caused the axial compression of the sprays. The fuel in spray leading edge with lower speed suggests that injection pressure in the early stage was much lower than that in the later stage. Complicated dynamic characteristics during the spray propagation have been revealed by the x-ray diagnostic method.

ACKNOWLEDGMENTS:

This work and the use of the APS are supported by the U.S. Department of Energy, under contract W-31-109-Eng-38. We gratefully acknowledge the support of Rogelio Sullivan, the SIDI program manager at OTT/DOE, for his faith and management. The authors wish to acknowledge the assistance from Raj Sekar. We thank Tim Mooney, Kurt Goetze of APS for their support during the experiments.

NOMENCLATURE

I	Transmitted x-ray intensity
I_0	Incident x-ray intensity
ρ	Fuel density (did we use this?)
μ_M	Linear absorption coefficient
M	Mass of fuel in the path of the beam
x	Coordinate along the spray axis
y	Coordinate perpendicular to the spray axis
z	Coordinate along the x-ray beam

REFERENCES

1. L.G. Dodge, SAE paper, No. 962015, 1996.
2. T. Kume, Y. Iwamoto, K. Iida, M. Murakami, K. Akishino, H. Ando, SAE Paper No. 960600, 1996
3. B. Chehroudi, S.H. Chen, and F.V. Bracco, SAE Paper, No. 850126, 1985.
4. W. Lawrence, SAE Paper, No. 960108, 1996.
5. H. Kosaka and T. Kamimoto, SAE Paper, No. 932653, 1993.
6. P.G. Felton, F.V. Bracco, and M.E.A. Bardsley, SAE Paper, No. 930870, 1993.
7. E. Sheid, F. Pischinger, K.F. Knoche, H.J. Daams, E.P. Hassel, and U. Reuter, SAE Paper, No. 861121, 1986.
8. D.L. Siebers, SAE Paper, No. 980809, 1998.
9. R. Tatschl, SAE Paper, No. 981464, 1998.
10. H. Hiroyas, Proceedings of ICLASS-91, Keynote Lecture, 1991, pp. 17-32.
11. C. F. Powell, Y. Yue, R. Poola and J. Wang, *Journal of Synchrotron Radiation*. 2000, 7, pt. 6, pp.356-360
12. C.F. Powell, Y. Yue, R. Poola, J. Wang, M.-C. Lai, J. Schaller, SAE 2001-01-0531, 2001,.
13. Yong Yue, Christopher F. Powell, Ramesh Poola, Jin Wang, Ming-Chia Lai, Scott E. Parrish, SAE 2001-01-1293, 2001
14. R. Poola, C. F. Powell, Y. Yue, S. Gupta, A. McPherson, and J. Wang, *8th International Conference on Liquid atomization and spray systems. June 2000, Pasadena, CA, USA*